

Optical investigation of the charge-density-wave phase transitions in NbSe₃

A. Perucchi,¹ L. Degiorgi,^{1,2} and R. E. Thorne³

¹Laboratorium für Festkörperphysik, ETH Zürich, CH-8093 Zürich, Switzerland

²Paul Scherrer Institute, CH-5232 Villigen, Switzerland

³Department of Physics, Cornell University, Ithaca, New York 14853, USA

(Received 14 January 2004; revised manuscript received 16 March 2004; published 28 May 2004)

We have measured the optical reflectivity $R(\omega)$ of the quasi-one-dimensional conductor NbSe₃ from the far infrared up to the ultraviolet between 10 and 300 K using light polarized along and normal to the chain axis. We find a depletion of the optical conductivity with decreasing temperature for both polarizations in the mid- to far-infrared region. This leads to a redistribution of spectral weight from low to high energies due to partial gapping of the Fermi surface below the charge-density-wave transitions at 145 K and 59 K. We deduce the bulk magnitudes of the charge-density wave gaps and discuss the scattering of ungapped free charge carriers and the role of fluctuation effects.

DOI: 10.1103/PhysRevB.69.195114

PACS number(s): 78.20.-e, 71.30.+h, 71.45.Lr

Quasi-one-dimensional linear-chain metals exhibit important deviations from Fermi liquid behavior and unusual phenomena associated with charge- and spin-density-wave broken symmetry ground states.^{1,2} A charge-density-wave (CDW) forms via a Peierls transition, in which an instability of the metallic Fermi surface (FS) due to nesting at $q=2k_F$ (k_F being the Fermi wave vector) couples to the Kohn anomaly in the phonon spectrum.³⁻⁵ As in conventional superconductivity the electron-phonon coupling is the dominant interaction,¹ and the transition leads to opening of a charge gap.

The transition-metal trichalcogenides MX_3 with $M = \text{Nb, Ta, Ti}$, and $X = \text{S, Se, Te}$ are among the most interesting materials displaying low dimensional electronic properties. Their crystallographic structure is made up of infinite chains of trigonal prisms.¹ The most remarkable properties have been observed in NbSe₃, which shows the phenomena of density wave transport cleanly than any other known system.¹ The resistivity remains metallic down to low temperatures, but two CDW phase transitions occur at $T_1 = 145$ K and $T_2 = 59$ K where the resistivity shows a sharp increase.⁶ Tight-binding calculations⁷ have shown that NbSe₃ has a primarily one-dimensional (1D) character with deviations due to the short intra- and interlayer Se-Se contacts. This transverse coupling produces a warped Fermi surface so that imperfect nesting and only partial gapping are expected.

The transition at T_1 is associated with a linear nesting, the wave vector of the CDW condensate pointing along the main chain axis, and the one at T_2 with a diagonal nesting.^{5,8} The literature values for the energy gaps, obtained by surface-sensitive techniques including point-contact, tunneling, and angle-resolved photoemission (ARPES) spectroscopies,⁹⁻¹³ vary significantly: $2\Delta_1 \sim 110-220$ meV for the T_1 CDW, and $2\Delta_2 \sim 40-90$ meV for the T_2 CDW. In all cases the gap values yield a ratio $2\Delta_i/k_B T_i$ much larger than the mean-field value of 3.52, and the mean-field transition temperature T_{MF} is much larger than the measured T_1 and T_2 . These discrepancies from mean-field values indicate the importance of one-dimensional fluctuations.

In principle, optical spectroscopic methods are an ideal

bulk-sensitive¹⁴ tool in order to investigate the CDW phase transitions.¹ Previous optical spectroscopy measurements were performed at room temperature¹⁵ or over an insufficient energy range^{16,17} which led to an erroneous evaluation of the CDW gaps. We provide here the first comprehensive study of the optical properties of NbSe₃ over a broad spectral range and as a function of temperature. The optical conductivity shows a redistribution of spectral weight from low to high frequencies with decreasing temperature, which we use to determine the bulk CDW (pseudo)gaps. We also observe precursor effects of the CDW phase transitions and establish that the resistivity anomalies are primarily the consequence of a Fermi-surface gapping and not due to changes in the lifetime of the charge carriers.

High-purity samples were grown as previously described.¹⁸ This study was made possible by preparing aligned mosaic specimens consisting of several wide, flat NbSe₃ ribbons with a resulting optical surface 3 mm long \times 2 mm wide. The optical reflectivity $R(\omega)$ was measured from the far infrared up to the ultraviolet between $T = 300$ K and 10 K. Polarizations along and transverse to the chain b axis were used to assess the anisotropic electrodynamic response. In our experiments, we paid great attention to the alignment of the specimens in our mosaic configuration. Different mosaics gave equivalent results. Moreover, and more importantly, we have mounted the specimen in such a way to have the chain axis always parallel with the polarization of light along the main cryostat axis. This way, we can prevent that undesired projections of the light polarization affect our data. The specimens were then coated with a 3000 Å gold layer and measured again, allowing correction for surface scattering from our mosaic samples without altering the overall shape and features of the spectra. Additional experimental details are described elsewhere.^{2,19} Kramers-Kronig transformations were used to calculate the real part $\sigma_1(\omega)$ of the optical conductivity. Standard high-frequency extrapolations $R(\omega) \sim \omega^{-s}$ (with $2 < s < 4$) were employed¹⁹ in order to extend the data set above 10^5 cm⁻¹ and into the electronic continuum. Because of scatter in the data at low frequencies (below 50 cm⁻¹), $R(\omega)$ was extrapolated using the Hagen-Rubens (HR) law $R(\omega) = 1 - 2\sqrt{(\omega/\sigma_{dc})}$ from

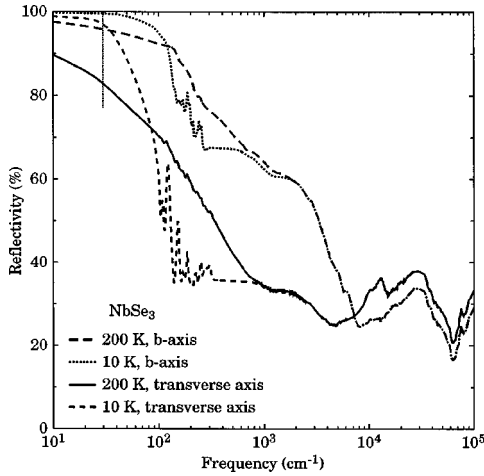


FIG. 1. Optical reflectivity $R(\omega)$ in NbSe_3 along both polarization directions and at two selected temperatures (10 and 200 K). The thin dotted line marks the frequency below which the Hagen-Rubens extrapolation has been performed.

data points in the $30\text{--}70\text{ cm}^{-1}$ range. This extrapolation yielded σ_{dc} values in agreement with dc transport data.^{6,20} The temperature dependence of $\sigma_1(\omega)$ is not affected by the details of this low-frequency extrapolation.

Figure 1 shows the optical reflectivity at two selected temperatures. It is metallic at all temperatures and for both polarization directions, but there is a remarkable anisotropy between the two crystallographic directions. Our $R(\omega)$ values qualitatively agree with previous yet partial reflectivity data in the respective common spectral ranges; our $R(\omega)$ spectra are considerably larger than $R(\omega)$ reported in Ref. 16, comparable to the spectra of Ref. 17 but somehow smaller than those in Ref. 15. For light polarized along the b axis the $R(\omega)$ plasma edge has a sharp onset around 1 eV ($\sim 8000\text{ cm}^{-1}$), while along the transverse axis a much more gradual and broad onset begins at about 0.5 eV ($\sim 4000\text{ cm}^{-1}$). $R(\omega)$ along the transverse axis resembles the so-called overdamped behavior¹⁹ typically seen in low dimensional systems² and may indicate incoherent charge transport along this direction. Previous $R(\omega)$ data¹⁵ at 300 K and over a smaller spectral range also showed anisotropic behavior. At low temperatures, $R(\omega)$ for both polarizations is depleted in the far and mid-infrared spectral range, but both show a sharp upturn at low frequencies. This upturn leads to a crossing of the 200 K and 10 K spectra around 100 cm^{-1} (well within the measured spectral range in Fig. 1) so that $R(\omega)$ increases with decreasing temperatures in the $\omega \rightarrow 0$ limit. Our 10 K data for light polarized along the b axis bear some similarities with earlier results at 2 K of Challaner and Richard¹⁶ which only covered the far infrared range ($\omega < 400\text{ cm}^{-1}$).

Figure 2 shows the temperature dependence of $\sigma_1(\omega)$ below 4000 cm^{-1} . Above 4000 cm^{-1} several absorptions (not shown here) ascribed to electronic interband transitions¹⁵ are observed. In the infrared spectral range, $\sigma_1(\omega)$ for both polarizations shows a rather strong mid-infrared band at 2000 cm^{-1} along the b axis and at 3000 cm^{-1} along the transverse axis. The low-frequency sides of these latter ab-

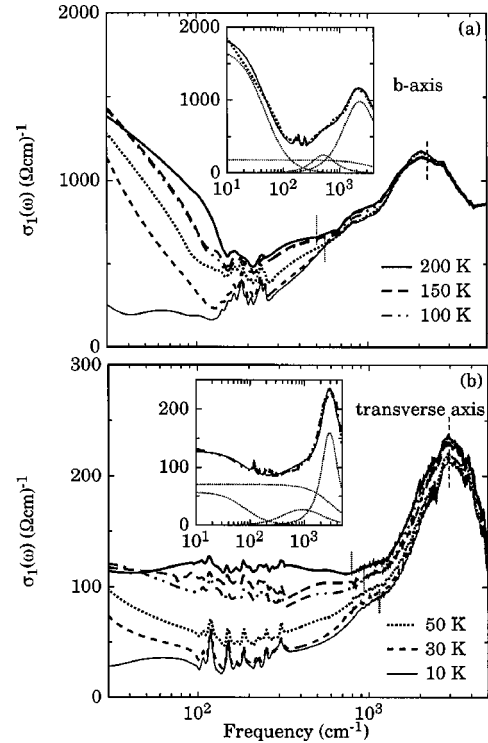


FIG. 2. Real part $\sigma_1(\omega)$ of the optical conductivity above 30 cm^{-1} as a function of temperature along (a) the chain b axis and (b) the transverse axis. The frequencies of the harmonic oscillators used to fit the two mid-infrared absorptions (see text) are indicated by thin dotted and dashed lines for the broad shoulder and the peak feature in $\sigma_1(\omega)$, respectively. The insets show the data at 50 K (b axis) and 100 K (transverse axis) with the total fit and its components.

sorptions for both axes have broad shoulders located below about 1000 cm^{-1} . There is an obvious suppression of spectral weight in the infrared range with decreasing temperature, while the effective (Drude) metallic component in the far infrared shifts to lower frequency and narrows. The narrowing of $\sigma_1(\omega)$ at low frequencies and temperatures follows from the steep increase of $R(\omega)$ around 100 cm^{-1} in Fig. 1. At low temperatures the narrowing is so strong that the spectral weight of the effective (Drude) metallic component falls entirely below our data's low-frequency limit. This leads to an apparent disagreement in Fig. 2 between $\sigma_1(\omega \rightarrow 0)$ and σ_{dc} , which results from the HR extrapolation used for $R(\omega)$ below 50 cm^{-1} .

In order to better highlight the relevant energy scales and in particular to address the redistribution of spectral weight versus temperature in $\sigma_1(\omega)$ and its connections with the CDW transitions in NbSe_3 , we have applied the phenomenological Lorentz-Drude (LD) approach based on the classical dispersion theory.¹⁹ For both polarization directions, the high-frequency response is fitted using Lorentz harmonic oscillators (ho) to describe the high-frequency electronic interband transitions. The low-frequency response can be fitted with two Drude terms and two mid-infrared ho's at about 561 and 2270 cm^{-1} for the b axis and at about 1100 and 2920 cm^{-1} for the transverse axis (inset of Fig. 2). The two

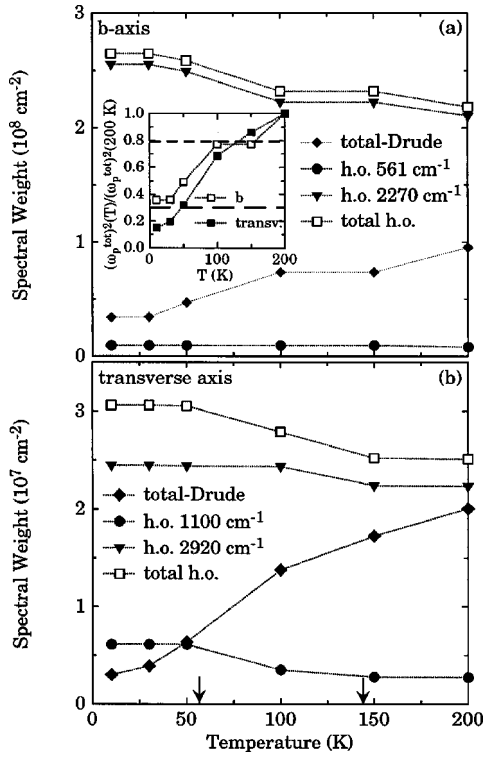


FIG. 3. Temperature dependence of the total spectral weight of the Drude terms and of the mid-infrared Lorentz harmonic oscillators, as well as of the spectral weights for the individual harmonic oscillators (a) along the chain b axis and (b) along the transverse axis. The CDW transition temperatures are indicated by arrows. The inset in (a) shows the normalized change of the total Drude weight $(\omega_p^{\text{tot}})^2$ with temperature, attributed to the gapping of the Fermi surface, for both axes. The dashed horizontal lines indicate the percentage of the Fermi surface which survives well below each of the two CDW transitions as determined by magnetotransport measurements (Ref. 6).

Drude terms could represent two conduction bands²⁰ that are both affected by the CDW transitions. Sharp Lorentz ho's are used to fit the IR-active phonon modes which appear with decreasing temperature.¹⁶ These modes contribute only a tiny fraction of the spectral weight in agreement with a previous infrared study of NbSe₃ (Ref. 16). These phonons acquire mode strength particularly below 100 K. Therefore, they might be likely phase phonons^{21,22} arising from the coupling between the lattice and the CDW condensate, as first suggested by Ref. 16. With this minimum set of Lorentz and Drude terms, we obtain an outstanding fit to $\sigma_1(\omega)$ at all temperatures.²³

Figure 3 shows how the spectral weight is redistributed among the Drude and mid-infrared Lorentz terms as temperature decreases. Both Drude terms lose spectral weight (i.e., the corresponding plasma frequency decreases) with decreasing temperature. For both polarization directions, the broad Drude term (see inset of Fig. 2) tends to lose first spectral weight (i.e., at $T < 150$ K) than the narrow one for which the suppression of weight occurs at $T < 70$ K. This is explicitly shown in Fig. 4. The resulting total Drude weight progressively decreases with decreasing temperature, with a

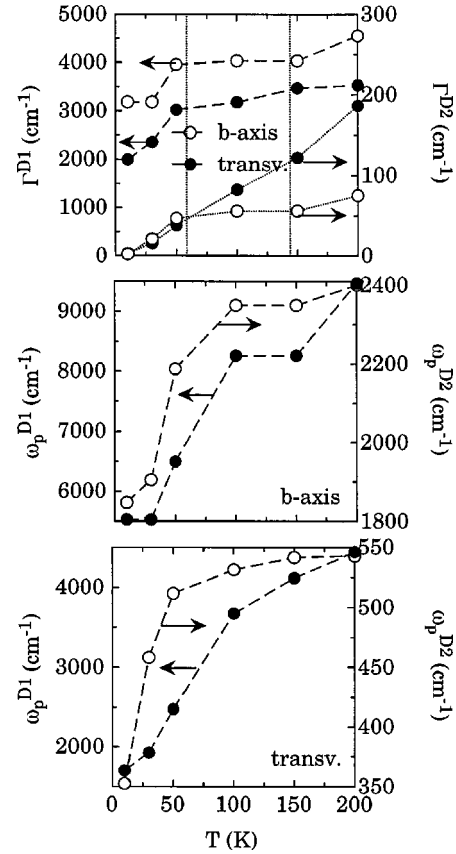


FIG. 4. Panel (a) shows the temperature dependence of the scattering rates for the first (D1, left y-axis scale) and second (D2, right y-axis scale) Drude term in the fits to both polarization directions. Solid symbols refer to the transverse axis and open ones to the b axis. The CDW transition temperatures are indicated by thin dotted lines. Panels (b) and (c) display the temperature dependence of the plasma frequencies for both Drude terms along the chain and the transverse direction, respectively.

more pronounced loss occurring below 100 K. The suppressed Drude weight is transferred to high energies and in particular to the mid-infrared absorptions, for both polarization directions. Along the b axis the harmonic oscillator at $\sim 2270 \text{ cm}^{-1}$ acquires most of the transferred weight, while along the transverse axis both absorptions gain weight. Part of the transverse axis weight is transferred to even higher energies and into the electronic continuum. Nevertheless, the total spectral weight $[\int_0^\infty \sigma_1(\omega) d\omega]$ for both polarization directions is fully recovered by 10^4 cm^{-1} ($\sim 1 \text{ eV}$), satisfying the optical sum rule. In this regard NbSe₃ closely resembles the 2H-XSe₂ dichalcogenides,²⁴ and does not show the “sum rule violation” of the high-temperature superconductors since the nature of the correlations in the two ground states are different.^{24,25}

The depletion of the Drude spectral weight in $\sigma_1(\omega)$ with decreasing temperature indicates a progressive gapping of the Fermi surface, which gets partially destroyed at the Peierls transitions. The inset of Fig. 3(a) shows the fraction change of the total Drude weight for both directions as a function of temperature. Ong and Monceau⁶ estimated from

transport data that approximately 20% of FS is destroyed at T_1 , while 62% of the remaining 80% is destroyed by gaps at T_2 . The corresponding values of residual ungapped Fermi surface are marked by dashed lines in the inset to Fig. 3(a), and are in excellent agreement with the present results for the b axis. We attribute the harmonic oscillator at 2270 cm^{-1} (281 meV) to the T_1 CDW gap²⁶ associated with linear nesting along the chain b axis, and the oscillator at 561 cm^{-1} (70 meV) to the T_2 CDW gap associated with the diagonal nesting.^{8,12} In transverse axis data, the CDW gap due to linear nesting should not be observable in our spectra (i.e., the transition probability is zero), so we attribute the harmonic oscillator at 1100 cm^{-1} (136 meV) to the CDW gap associated with the diagonal nesting. This suggests anisotropic gapping for the diagonal nesting.¹³ The optical gaps compare well with the broad interval of gap estimates from tunneling, point-contact, and ARPES spectroscopy.⁹⁻¹³ Our estimated (direct) optical CDW gaps are larger than the indirect gaps obtained from tunneling.⁹⁻¹¹ Deviations from the k -resolved ARPES findings^{8,12} may arise in part because optical measurements average over the k space. Additional deviations may result because of differences between the bulk optical value and the near-surface value probed by these other techniques. Our gap value for the T_2 CDW transition and for light polarized along b is a factor of 3 to 4 larger than the estimate¹⁶ of $120\text{--}190\text{ cm}^{-1}$ (15–24 meV) obtained in the first and only other optical study at low temperature of NbSe₃. At the time of these earlier measurements the large ratio $2\Delta/k_B T$ characteristic of these materials was not recognized, and so data collection did not extend much beyond energies corresponding to the measured T_2 and the mean-field ratio. Our transverse axis $\sigma_1(\omega)$ data and LD analysis indicate the presence of another absorption at about 2920 cm^{-1} (362 meV). This energy is too large to be ascribed to a CDW gap,^{9-13,15,16} and likely arises from the band structure. It may be a hybridizationlike gap induced by Brillouin-zone backfolding arising from the Fermi-surface nesting.⁸

The chain and transverse axis absorptions at 561 and 1100 cm^{-1} , respectively (thin dotted lines in Fig. 2), decreases with increasing temperature, though in a moderate fashion. In strict one-dimensional systems, like the well-known blue-bronze K_{0.3}MoO₃, the metal-insulator CDW transition leads to a complete transfer of the Drude spectral weight into the CDW gap feature, leading to the formation of a peak at the gap energy.²² The formation of the peak in the optical conductivity at the gap is also the consequence of the so-called coherence factors.¹⁹ The imperfect nesting of NbSe₃ and its metallic character down to low temperatures

lead to a less intensive peak for the CDW gaps in $\sigma_1(\omega)$. Such a situation is even more pronounced in the more two-dimensional dichalcogenides materials.²⁴

The mid-infrared absorptions persist to temperatures well above T_1 and T_2 , a quite common situation in CDW systems.¹ This provides evidence for the importance of 1D fluctuations²⁷ in the regime between the measured transition temperatures and the much larger T_{MF} . Evidence for these fluctuations has previously been obtained in x-ray diffraction,⁴ ARPES,^{8,12} and tunneling experiments.¹⁰ In light of these strong fluctuation effects, the mean-field or BCS-like form of the temperature dependence of the CDW gap observed in x-ray diffraction⁵ and point-contact spectroscopy experiments¹³ remains puzzling. Nevertheless, the BCS scenario is far from being widely accepted in the literature. In this respect, there is a wealth of contradictory results in NbSe₃, even from experiments employing the same technique.

Finally, we discuss the scattering rates (Γ) for the Drude terms (Fig. 4). The Γ value for the first (narrow) Drude term is partially determined by the HR extrapolation of $R(\omega)$. However, its temperature dependence is strikingly similar to that of Γ for the second (broad) Drude term, which covers an extended spectral range going well beyond the range of the HR extrapolation, suggesting that the extrapolation is not responsible for the observed behavior. As directly indicated by the narrowing of $\sigma_1(\omega)$ with decreasing temperature, the scattering rates show a pronounced drop below 50 K for both Drude terms and both polarization directions. As in the two-dimensional 2H-XSe₂ dichalcogenide systems²⁴ this clearly indicates that some scattering channels freeze out when the long-range-ordered CDW condensate develops. On the other hand, short-range ordered CDW segments present for temperatures $T > T_2$ can lead to additional scattering of the ungapped charge carriers. The weak temperature dependence of Γ above T_2 reinforces the notion²⁰ that the (CDW) resistivity anomalies are due to changes in the carrier concentration [inset of Fig. 3(a)] and not in the lifetime.

In conclusion, we have performed the first complete and bulk sensitive optical investigation of NbSe₃. We identify the energy scales associated with the CDW gaps, determine the fractional gapping of the Fermi surface, observe CDW fluctuation effects above the experimental Peierls transitions, and establish the suppression of the free charge carriers scattering in the broken symmetry ground state.

The authors wish to thank J. Müller for technical help, and R. Claessen, J. Schäfer, and M. Gioni for fruitful discussions. This work was supported by the Swiss National Foundation for the Scientific Research and by the NSF (Grant No. DMR-0101574).

¹G. Grüner, *Density Waves in Solids* (Addison-Wesley, Reading, MA, 1994), and references therein.

²V. Vescoli, F. Zwick, W. Henderson, L. Degiorgi, M. Gioni, G. Grüner, and L.K. Montgomery, *Eur. Phys. J. B* **13**, 503 (2000).

³J.P. Pouget and R. Comes, in *Charge Density Waves in Solids*, edited by L.P. Gor'kov and G. Grüner (North Holland,

Amsterdam, 1989), p. 85.

⁴A.H. Moudden, J.D. Axe, P. Monceau, and F. Levy, *Phys. Rev. Lett.* **65**, 223 (1990); S. Rouzière, S. Ravy, J.P. Pouget, and R.E. Thorne, *Solid State Commun.* **97**, 1073 (1996).

⁵R.M. Fleming, D.E. Moncton, and D.B. McWhan, *Phys. Rev. B* **18**, 5560 (1978).

- ⁶N.P. Ong and P. Monceau, *Phys. Rev. B* **16**, 3443 (1977).
- ⁷E. Canadell, I.E.-I. Rachidi, J.P. Pouget, P. Gressier, A. Meerschaut, J. Rouxel, D. Jung, M. Evain, and M.-H. Whangbo, *Inorg. Chem.* **29**, 1401 (1990).
- ⁸J. Schäfer, Eli Rotenberg, S.D. Kevan, P. Blaha, R. Claessen, and R.E. Thorne, *Phys. Rev. Lett.* **87**, 196403 (2001).
- ⁹T. Ekino and J. Akimitsu, *Physica B* **194-196**, 1221 (1994).
- ¹⁰Z. Dai, C.G. Slough, and R.V. Coleman, *Phys. Rev. Lett.* **66**, 1318 (1991); H. Haifeng and Z. Dianlin, *ibid.* **82**, 811 (1999).
- ¹¹A. Fournel, J.P. Sorbier, M. Konczykowski, and P. Monceau, *Phys. Rev. Lett.* **57**, 2199 (1986).
- ¹²J. Schäfer, M. Sing, R. Claessen, Eli Rotenberg, X.J. Zhou, R.E. Thorne, and S.D. Kevan, *Phys. Rev. Lett.* **91**, 066401 (2003).
- ¹³A.A. Sinchenko and P. Monceau, *Phys. Rev. B* **67**, 125117 (2003).
- ¹⁴In the classical skin depth regime, literature values of the resistivity (Ref. 20) lead to penetration depth of the IR radiation of about 2000 Å.
- ¹⁵H.P. Geserich, G. Scheiber, F. Lévy, and P. Monceau, *Physica B & C* **143B**, 174 (1986); *Solid State Commun.* **49**, 335 (1984).
- ¹⁶W.A. Challaner and P.L. Richard, *Solid State Commun.* **52**, 117 (1984).
- ¹⁷J. Nakahara, T. Taguchi, T. Araki, and M. Ido, *J. Phys. Soc. Jpn.* **54**, 2741 (1985).
- ¹⁸R.E. Thorne, *Phys. Rev. B* **45**, 5804 (1992).
- ¹⁹F. Wooten, *Optical Properties of Solids* (Academic Press, New York, 1972); M. Dressel and G. Grüner, *Electrodynamics of Solids* (Cambridge University Press, Cambridge, 2002).
- ²⁰N.P. Ong and J.W. Brill, *Phys. Rev. B* **18**, 5265 (1978); N.P. Ong, *ibid.* **18**, 5272 (1978).
- ²¹M.J. Rice, *Phys. Rev. Lett.* **37**, 36 (1976).
- ²²L. Degiorgi, B. Alavi, G. Mihály, and G. Grüner, *Phys. Rev. B* **44**, 7808 (1991).
- ²³Different fit procedures with variable number of fit components were considered but yielded equivalent results. The temperature dependence of the extracted parameters and above all the redistribution of spectral weight unambiguously converge to a unique trend. The complete set of fit parameters can be load down from the link: <http://www.solidphys.ethz.ch/spectro/suppinfo/NbSe3-fit=param.pdf>
- ²⁴S.V. Dordevic, D.N. Basov, R.C. Dynes, B. Ruzicka, V. Vescoli, L. Degiorgi, H. Berger, R. Gaál, L. Forró, and E. Bucher, *Eur. Phys. J. B* **33**, 15 (2003).
- ²⁵L.B. Ioffe and A.J. Millis, *Science* **285**, 1241 (1999).
- ²⁶Because of the remaining Fermi surface and Drude weight the CDW single-particle excitations should be correctly named as pseudogaps. For simplicity we call them CDW gaps.
- ²⁷A. Schwartz, M. Dressel, B. Alavi, A. Blank, S. Dubois, G. Grüner, B.P. Gorschunov, A.A. Volkov, G.V. Kozlov, S. Thieme, L. Degiorgi, and F. Lévy, *Phys. Rev. B* **52**, 5643 (1995).